

## Supporting Information

# Sulfide Cluster Vacancy Inducing an Electrochemical Reversibility Improvement of Titanium Disulfide Electrode Material

Jianhao Lu<sup>a</sup>, Fang Lian<sup>a\*</sup>, Yuxuan Zhang<sup>a</sup>, Ning Chen<sup>a</sup>, Yang Li<sup>b</sup>, Fei Ding<sup>b</sup>, Xinjiang Liu<sup>b\*</sup>

a School of Materials Science and Engineering, University of Science & Technology Beijing, Beijing 100083, PR China.

b Science and Technology on Power Sources Laboratory, Tianjin Institute of Power Sources, Tianjin 300384, PR China.

\*Corresponding author:

[a\\*E-mail: lianfang@mater.ustb.edu.cn](mailto:lianfang@mater.ustb.edu.cn).

[b\\*E-mail: xjliu@nklps.org](mailto:xjliu@nklps.org)

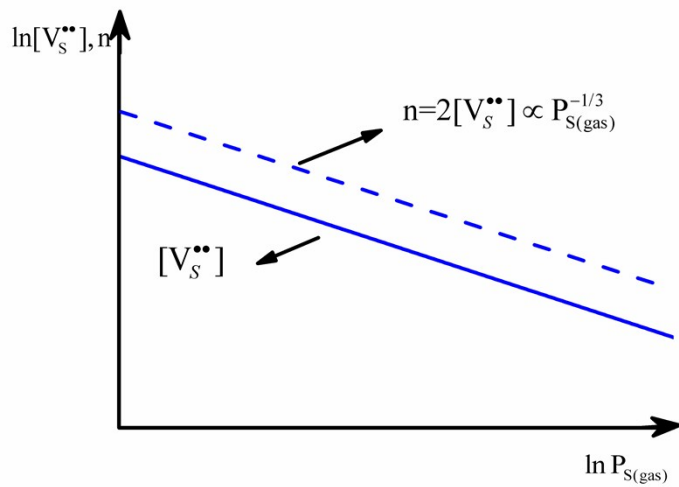


Fig. S1 A Plot of  $\ln[n]/\ln [V_S^{\bullet\bullet}]$ - $\ln P_{S(\text{gas})}$  (Brouwer diagramm)

The sulfur vacancies are denoted as  $[V_S^{\bullet\bullet}]$ , partial pressure of sulfur is  $P_{S(\text{gas})}$  and  $n$  is free electron. According to the equilibrium constant of vacancy reaction and neutral condition, the relationship between sulfur vacancy concentration and partial pressure of sulfur can be shown in the Fig. S1.

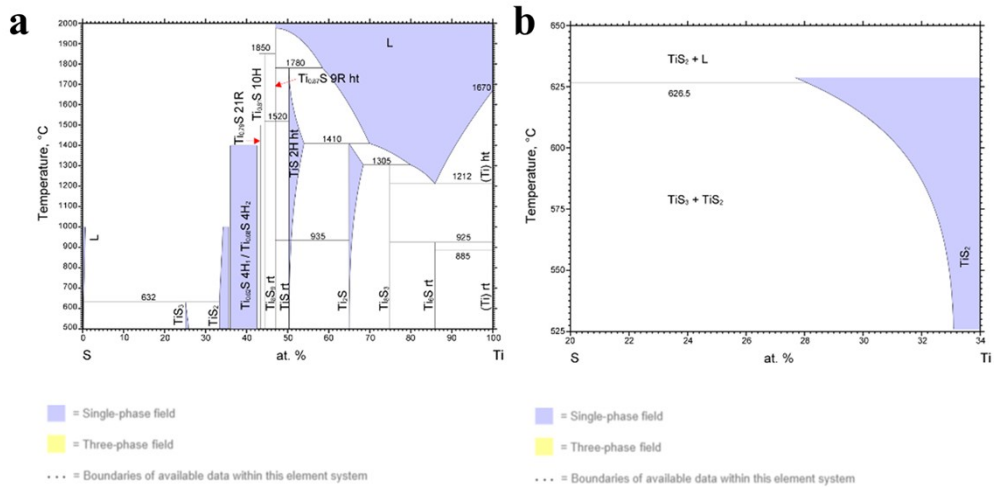


Fig. S2 S-Ti Binary Phase Diagram 0-100 at.% Ti (a); S-Ti Binary Phase Diagram 20-34 at.% Ti (b) (Springer.Materials)<sup>1-2</sup>.

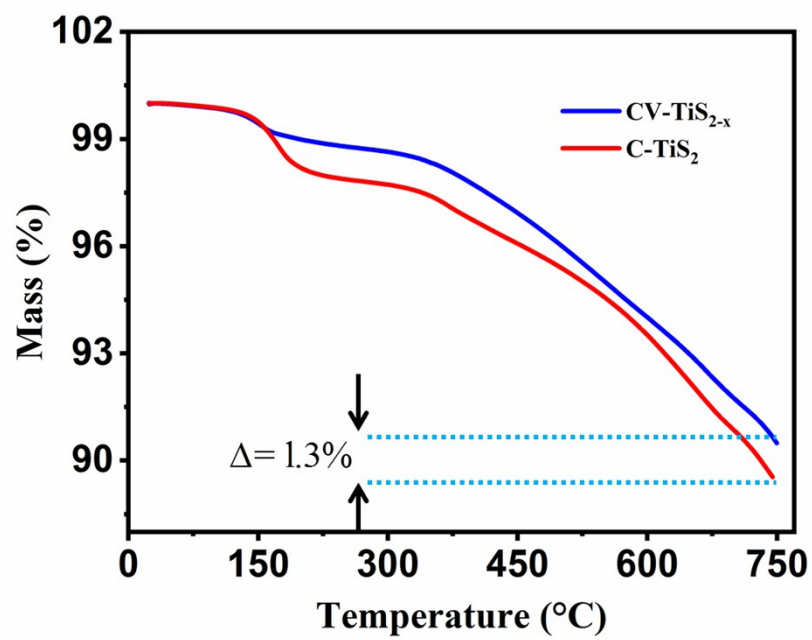


Fig. S3 TGA analysis of CV-TiS<sub>2-x</sub> and C-TiS<sub>2</sub>.

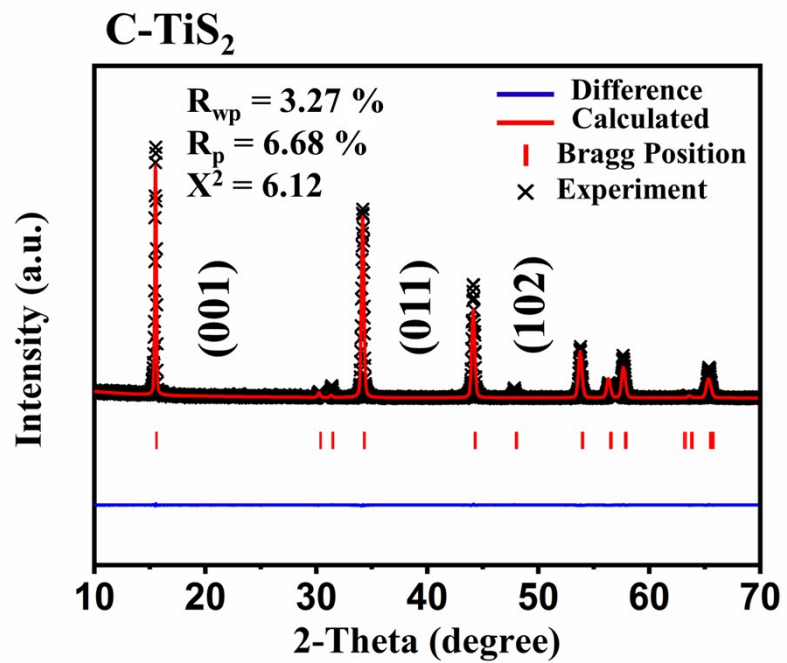


Fig. S4 The XRD pattern of C-TiS<sub>2</sub>.

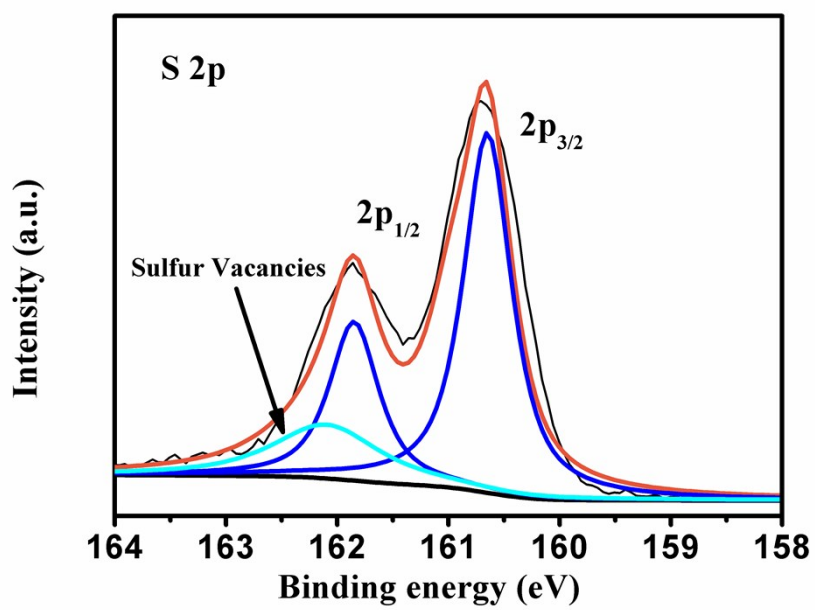


Fig. S5 S 2p XPS spectra regions for CV-TiS<sub>2-x</sub>.

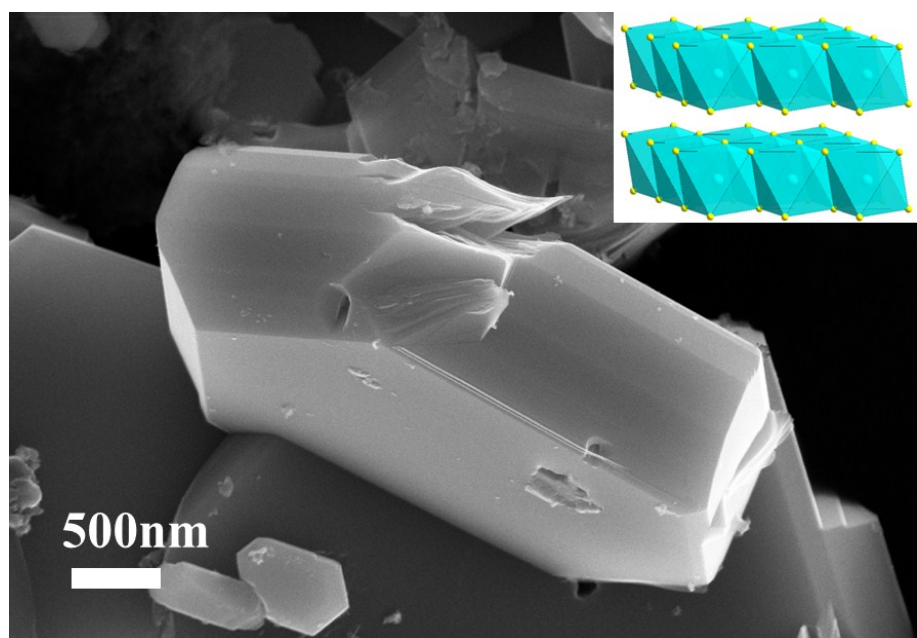


Fig. S6 SEM image of CV- $\text{TiS}_{2-x}$  with particle size larger than 500 nm.

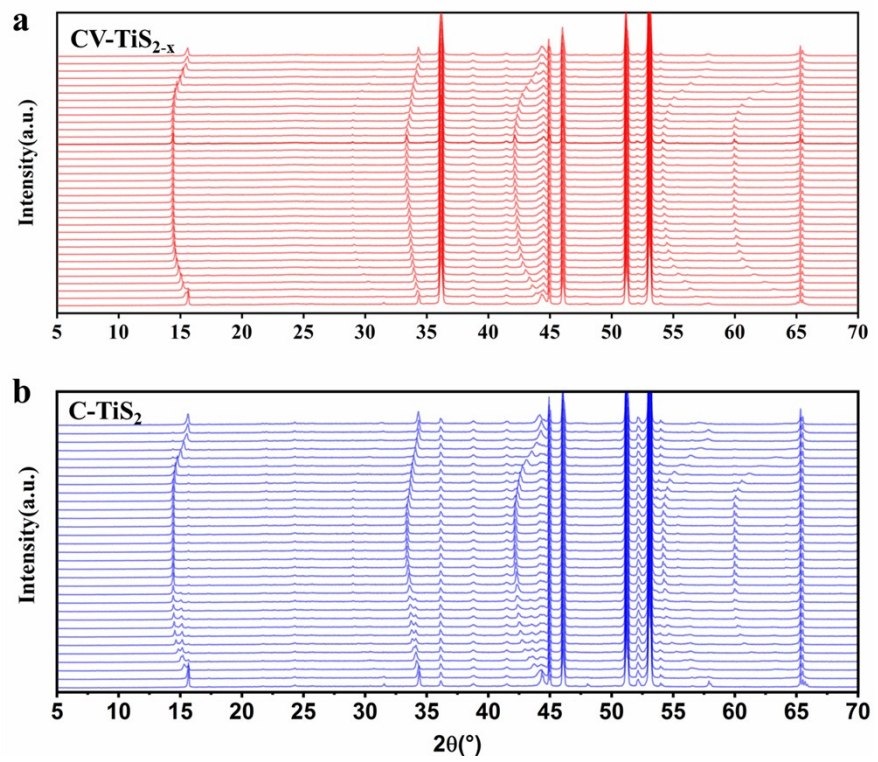


Fig. S7 In situ XRD patterns of CV-TiS<sub>2-x</sub> (a) and C-TiS<sub>2</sub> (b) electrodes during the initial cycle at 1C.

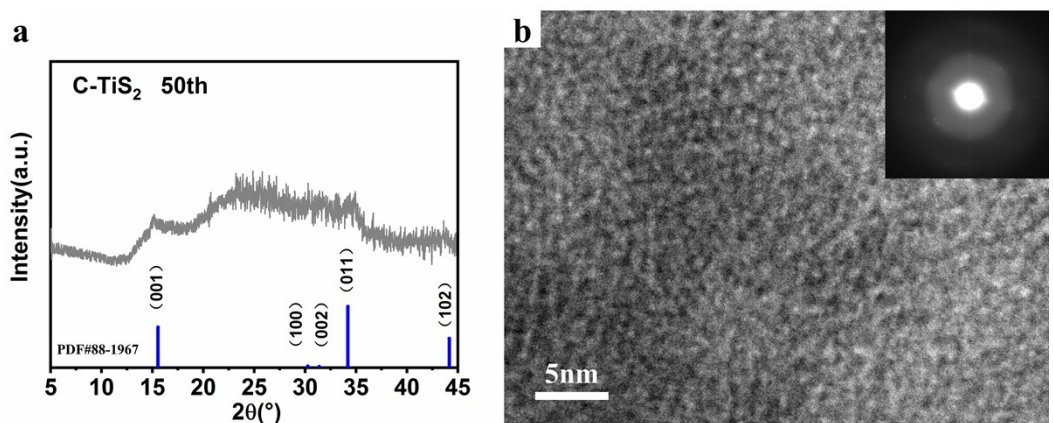


Fig. S8 XRD results of C-TiS<sub>2</sub> electrode after 50 cycles (a) and the corresponding TEM images (b).

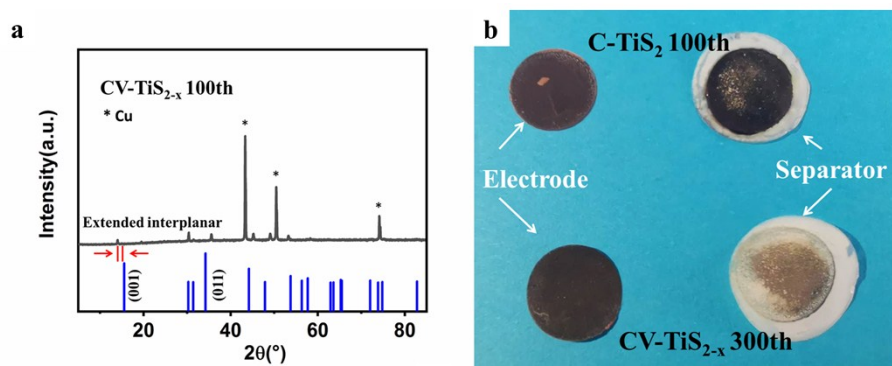


Fig. S9 XRD patterns of the CV-TiS<sub>2-x</sub> after 100 cycles (a). The electrodes and separators of C-TiS<sub>2</sub> and CV-TiS<sub>2-x</sub> batteries after cycling (b).

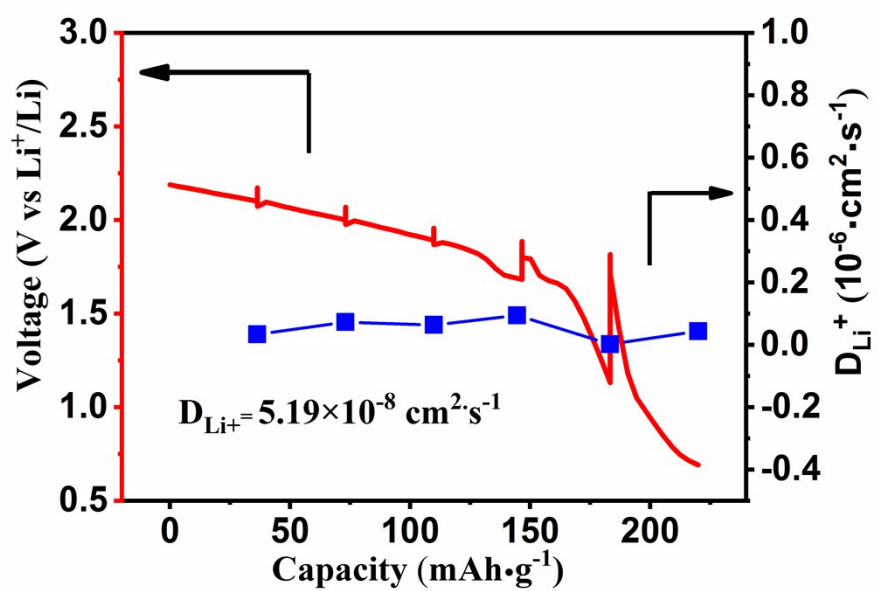


Fig. S10 GITT curves of C-TiS2 at the first cycle with a relaxation time of 2h.

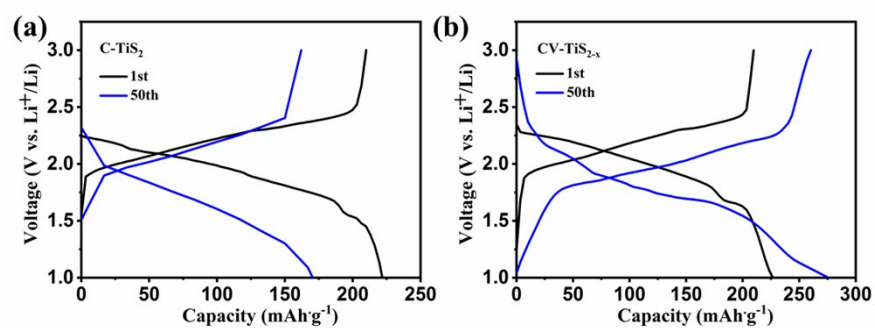


Fig. S11 Galvanostatic discharge / charge curves of CV-TiS<sub>2-x</sub> (a) and C-TiS<sub>2</sub>(b) electrode at a current density of 1C.

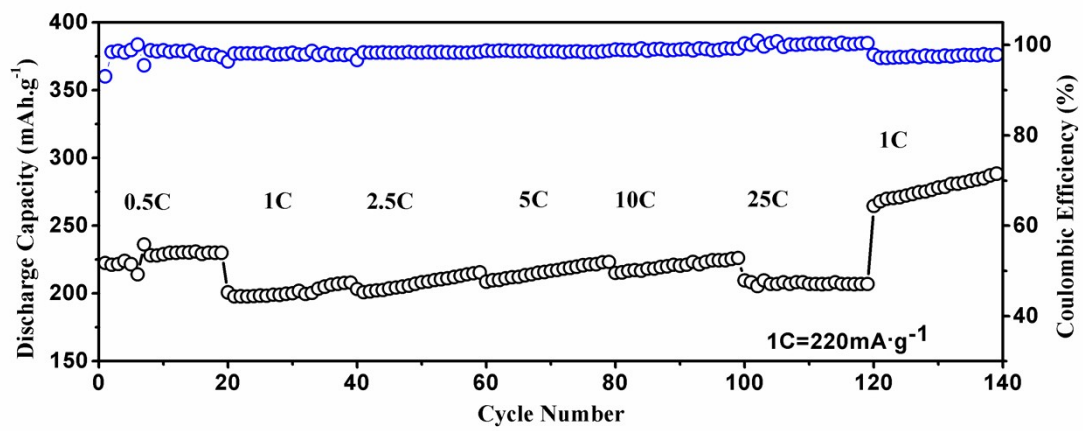


Fig. S12 The rate capability of CV-TiS<sub>2-x</sub> electrode (1C=220mA·g<sup>-1</sup>).

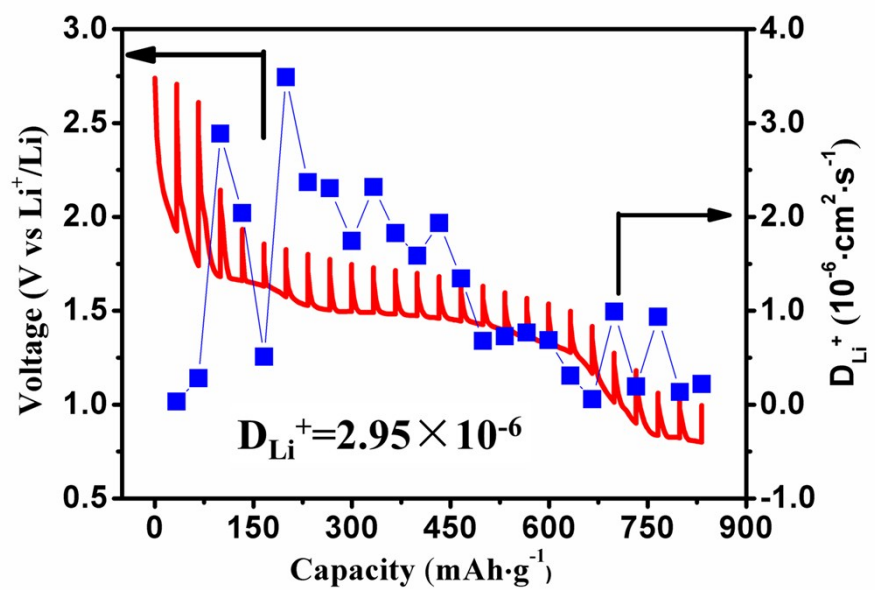


Fig. S13 GITT of CV-TiS<sub>2-x</sub> electrode in the 300th discharging at 25 °C.

Table S1. The molar ratio of Ti : S in C-TiS<sub>2</sub> and CV-TiS<sub>2-x</sub>

| Samples               | Ti : S molar ratio |                  |
|-----------------------|--------------------|------------------|
|                       | based on XPS       | based on ICP-OES |
| CV-TiS <sub>2-x</sub> | 1.87               | 1.82             |
| C-TiS <sub>2</sub>    | 2.15               | 1.97             |

In both samples, the XPS determined stoichiometry is significantly higher than the ICP-OES determined stoichiometry. As XPS only detects the surface of the material while ICP-OES detects the bulk, this suggests that the surface of the electrode materials is more sulfur rich than the interior.

Table S2 The lattice parameters of CV-TiS<sub>2-x</sub> and C-TiS<sub>2</sub>.

|                                  | CV-TiS <sub>2-x</sub> | C-TiS <sub>2</sub> |
|----------------------------------|-----------------------|--------------------|
| Lattice volume (Å <sup>3</sup> ) | 56.92                 | 56.98              |
| Lattice-substitution             | 0.97                  | 1.02               |
| Bond length (Å)                  | 2.412                 | 2.423              |

Table S3 Electrochemical performance comparison

| Chemical                    | Current ( $\text{mA}\cdot\text{g}^{-1}$ ) | Capacity ( $\text{mAh}\cdot\text{g}^{-1}$ ) | Reference |
|-----------------------------|---|---|-----------|
| CV-TiS <sub>2-x</sub>       | 220                                       | 650(300th)                                  | This work |
| TiS <sub>2-x</sub>          | 230                                       | 183(100th)                                  | [3]       |
| TiS <sub>2-x</sub> nanobelt | 23  | 224(100th)                                  | [4]       |
| TiS <sub>2</sub>            | 100                                       | 187(120th)                                  | [5]       |

## References

1. M. Onoda and H. Wada, Journal of the Less-Common Metals, 132, 0-207.
2. R. R. Chianelli, J. C. Scanlon and A. H. Thompson, Mater. Res. Bull., 10, 1379-1382.
3. C. G. Hawkins and L. Whittaker-Brooks, ACS Applied Nano Materials, 2018, 1, 851-859.
4. C. G. Hawkins and L. Whittaker-Brooks, Journal of Materials Chemistry A, 2018, 6, 21949-21960.
5. A. Chaturvedi, P. Hu, V. Aravindan, C. Kloc and S. Madhavi, Journal of Materials Chemistry A, 2017, 5, 9177-9181.